JOURNAL OF APPLIED ELECTROCHEMISTRY **28** (1998) 193–199

Potential instabilities of lead–silver alloy anodes in acidic sulfate electrolytes

C. CACHET, C. LE PAPE-RÉROLLE, R. WIART

UPR 15 du CNRS, Physique des Liquides et Électrochimie, Université Pierre et Marie Curie, Tour 22, 4 Place Jussieu, 75252 Paris Cedex 05, France

Received 4 March 1997; revised 25 May 1997

The kinetic behaviour of lead and lead–silver anodes, polarized under galvanostatic conditions in a H_2SO_4–$ZnSO_4$–$MnSO_4$ electrolyte, has been studied. Whereas the potential of the lead anode stabilizes during electrolysis, the potential of the lead–silver alloy anode oscillates between two limits after an induction time. Both silver on the anode surface and manganese in the electrolyte are required for the potential oscillations to appear. With increasing time the potential oscillations change in shape and period. From impedance data obtained earlier, at the beginning of, and during the potential oscillations, it is shown that the potential instabilities originate from electrode coverage by a silver salt adsorbate.

Keywords: *Pb and Pb–Ag anode*, *oxygen evolution*, *potential oscillations*, *impedance*, *inhibiting adsorbate*

1. Introduction

In electrochemical systems there are numerous examples of oscillatory behaviour appearing under potentiostatic or galvanostatic control [1–3]. Frequently, the oscillations have been associated with the presence of a passivating process able to generate a negative resistance in the electrode impedance. It is also known that a passivating process can generate multiple steady states, primarily when it is coupled with the other steps by diffusion [4].

During zinc electrowinning in acidic sulfate electrolytes, potential oscillations of the cathode potential have been observed which correspond to cycles of alternate zinc deposition and deposit redissolution [5]. These oscillations appear after an induction period and originate from the presence of metal impurities in the electrolyte, which codeposit on the electrode and stimulate hydrogen evolution [5–8]. In this case, the polarization curve recorded under potentiostatic conditions reveals a hydrogen peak and a more cathodic branch corresponding to zinc deposition. Between the hydrogen peak and the zinc deposition branch, there exists a potential region where the polarization resistance of the electrode is negative, due to a strong inhibition of hydrogen evolution [9].

During oxygen evolution on Pb–Ag alloy anodes in H_2SO_4–$ZnSO_4$–$MnSO_4$ electrolytes for zinc electrowinning, potentiostatic measurements of the electrode impedance have recently revealed an inhibiting process which slowly degenerates into a passivating process with increasing electrolysis time [10]. This passivating process has been ascribed to the formation of a silver salt adsorbed on the MnO_2 oxide layer [11], thus suggesting the possible occurrence of instabilities for this electrochemical system. However, the passivating process is fast, as compared to the inductive feature which governs the slope of the steady-state polarization curve, which remains single-valued without the presence of multistates.

The aim of the present work was to analyse the stability of Pb–Ag anodes polarized under galvanostatic conditions. In this paper, the existence of potential oscillations will be demonstrated and an interpretation of experimental results will be proposed.

2. Experimental details

2.1. *Electrodes and cell*

Anodes of pure lead (Johnson Matthey, specpure 99.9999%) and silver–lead alloys (Union-Minière, silver content 0.128% and 0.56%, other impurities given in Table 1) were used, with an effective surface area of 1 or 1.13 cm^2. They were vertically oriented in the cell and insulated with epoxide resin (Buehler). Before electrolysis, a mirror-like polish was achieved with emery paper (grit 1200).

To clarify the chemical influence of silver used as an alloying element, we also studied pure lead electrodes chemically preformed for 3 s in 0.3 M HNO_3 + 0.2 M $AgNO_3$ solution, so as to create a number of active silver sites on the anode surface.

The counter electrode was aluminium (Union-Minière) with an effective surface area of 1 cm^2 positioned in front of the working electrode surface. The reference electrode was a saturated Hg/Hg_2SO_4 electrode (SSE), and a magnetic stirring of electrolyte was realized. The electrolysis cell was thermostated at 37 °C and the electrolyte volume was approximately 200 cm^3.

Table 1. Impurity contents in Pb–Ag alloy (*Union Minière*)

Impurity /ppm	Bi	As	Sn	Fe	Cu	Sb	Zn	Cd
	< 250	< 1	< 1	< 8	< 12	< 1	< 5	< 10

The H_2SO_4–$ZnSO_4$–$MnSO_4$ electrolyte consists of 1.83 M H_2SO_4, 0.84 M $ZnSO_4$ and 0.091 M $MnSO_4$. All chemicals were Merck products of analytical grade purity and the water was doubly ion-exchanged and twice distilled in a quartz apparatus.

2.2. *Experimental methods*

The anodes were directly polarized under galvanostatic conditions near the industrial working point at a constant current of 50, or 80 mA cm^{-2}, and were maintained at this current. The variations $V(t)$ of the electrode potential were recorded as a function of time.

The electrolyte resistance, R_e, is known to characterize the screening effect of bubbles at the electrode surface [12–14] and fluctuations of R_e reflect their growth and detachment on the electrode [15, 16]. In the present work, the anode electrolyte resistance was obtained from the electrode impedance, measured at 20 kHz, every 14 s. R_e and V were recorded simultaneously.

Impedance measurements were performed using a frequency response analyser (Solartron 1250) and an electrochemical interface (Solartron 1280) controlled by an IBM PS/2 microcomputer. The signal amplitude was 3 mV.

3. Results and discussion

3.1. *Lead–silver alloy anodes*

The results obtained with Pb–Ag (0.128%) and Pb–Ag (0.56%) anodes, polarized at 50 or 80 mA cm^{-2} in the H_2SO_4–$ZnSO_4$–$MnSO_4$ electrolyte, were similar. In most cases the electrode potential was stable at the beginning of electrolysis, and started oscillating after a variable induction time. The amplitude and the two potential limits V_{min} and V_{max} were scattered from one experiment to another. In a few cases no oscillation (NO) appeared within the observation time of 25 h. Figures 1 and 2, respectively, show the statistical representation of the induction time necessary for the oscillations to appear, and of the oscillation amplitude, as functions of the experiment number. When oscillations appeared, the average induction time was 10 h of electrolysis and the mean oscillation amplitude was 110 mV: the average values of V_{min} and V_{max} were 1.38 and 1.49 V vs SSE, respectively. Taking into account the poor reproducibility of V_{min} and V_{max} values, it can be considered that the two types of Pb–Ag anode have the same polarization characteristics. For the same reason, it is difficult to make a difference between the results obtained at $i = 50$ mA cm^{-2} and $i = 80$ mA cm^{-2}.

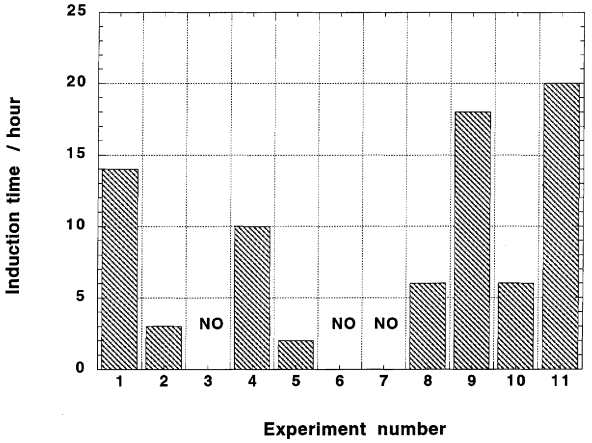

Fig. 1. Statistical representation of the induction time for the oscillations to appear, as a function of experiment number. NO means no oscillation.

After the induction time, potential oscillations appeared and progressively changed in shape and period with increasing time. This phenomenon is illustrated in Figs 3, 4 and 5, which present fluctuations of potential $V(t)$ and electrolyte resistance $R_e(t)$ for various electrolysis durations, at constant current density (50 mA cm^{-2}). From the beginning of electrolysis (Fig. 3), only small potential fluctuations due to oxygen bubbles were observed. Then the oscillations started after about 1 h. The increase in R_e is due to the slow formation of a duplex PbO_2–MnO_2 oxide layer, and probably reflects a change in the screening effect by bubbles. It is known that small bubbles evolve at the beginning of electrolysis on a major part of the electrode [10]. With increasing electrolysis time only the sites at the bottom of macropores in the MnO_2 layer remain active and oxygen has been observed to take place only by big bubbles evolving through a few holes in the outer MnO_2 layer [11]. In Fig. 3, the continuous increase in the ohmic drop, iR_e, was about 10 mV, which is consistent with the

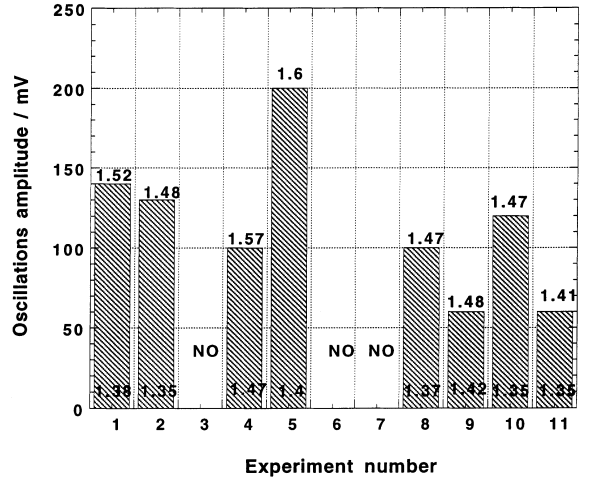

Fig. 2. Statistical representation of the oscillations amplitude as a function of experiment number. The potentials V_{min} and V_{max}, in volts vs SSE, are reported for each experiment. NO means no oscillation.

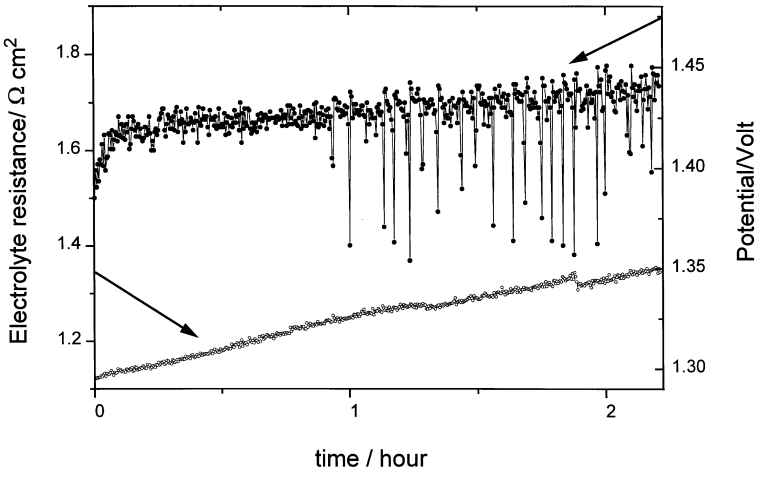

Fig. 3. Fluctuations of potential $V(t)$ and electrolyte resistance $R_e(t)$ from the beginning of electrolysis at $i = 50\,\mathrm{mA\,cm^{-2}}$.

slow drift of the potential, about 20 mV for 2 h of electrolysis. After several hours the potential V oscillated more periodically and the shape of the oscillations varied: the potential remained closer to V_{max} than to V_{min}, over a longer time, as illustrated in Fig. 4, which was obtained after 11 hours of electrolysis. Then the situation was reversed after 20 h, Fig. 5. Between these two situations, the bubble configuration probably changed, since the electrolyte resistance, R_e, decreased.

In Figs 4 and 5, no correlation appears between the potential oscillations of amplitude close to 100 mV and variations of $R_e(t)$ which induces variations in the ohmic drop $iR_e(t)$ of about 1 mV. On the other hand, a pure lead anode polarized under the same conditions never oscillated: the potential remained close to $V = 1.53$ V vs SSE. Consequently, it is clear that silver as alloying element is necessary to produce the potential oscillations.

3.2. *Lead anodes preformed in acidic $AgNO_3$ solution*

To better understand the influence of silver as an alloying element, pure lead anodes were chemically preformed in a $AgNO_3 + HNO_3$ solution. This treatment induces the creation of separate silver sites scattered on the anode surface, as shown in Fig. 6.

Figure 7 shows the $V(t)$ recording corresponding to one of these anodes polarized at $i = 80\,\mathrm{mA\,cm^{-2}}$ in the H_2SO_4–$ZnSO_4$–$MnSO_4$ electrolyte. The potential value, initially low ($V = 1.31$ V vs SSE) progressively increased with time to attain $V = 1.39$ V vs SSE after 1 h of electrolysis (Fig. 7 (a)). At this time, potential oscillations appeared and an amplitude of about 150 mV was attained for an electrolysis time of 8 h, Fig. 7(b). Therefore, when silver sites are present on the pure lead anode surface from the beginning of electrolysis, potential oscillations also appear. With the preformed anodes, the potential oscillations disappeared for long electrolysis times, Fig. 7(c), and then the mean potential value, $V = 1.53$ V vs SSE, corresponded to that of a pure lead anode. At this moment, there were probably no more silver sites on the performed anode surface, due to their anodic dissolution and/or their inclusion in the MnO_2 layer. The remaining potential fluctuations in Fig. 7(c) correspond to oxygen bubbles. These results show that the silver sites on the anode surface are directly involved in the existence of oscillations.

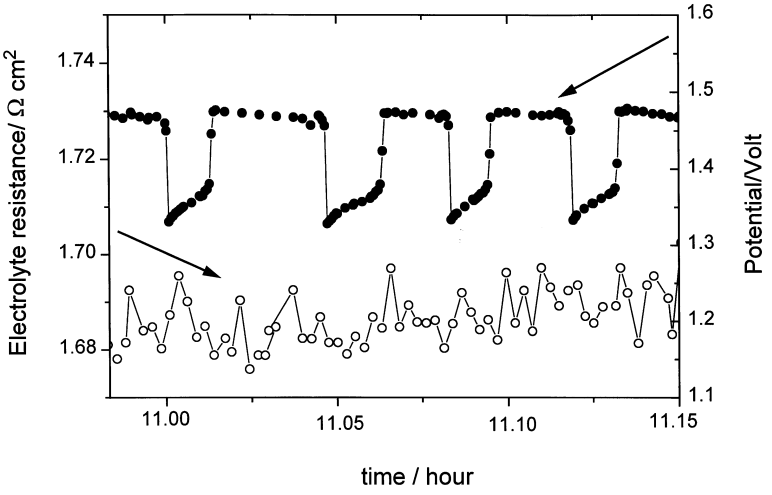

Fig. 4. Fluctuations $V(t)$ and $R_e(t)$ after electrolysis for 11 h. Same anode and conditions as for Fig. 3.

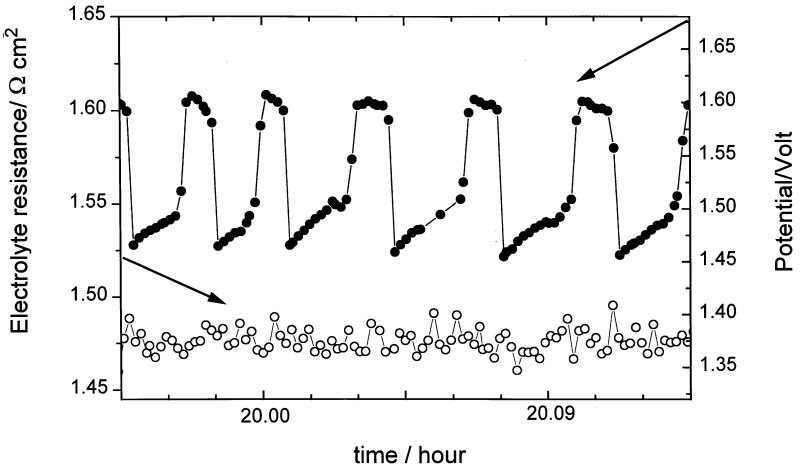

Fig. 5. Fluctuations $V(t)$ and $R_e(t)$ after electrolysis for 20 h. Same anode conditions as for Fig. 3.

Another pure lead anode, preformed in the same manner, was then polarized at $i = 80\,\mathrm{mA\,cm^{-2}}$ in a Mn^{2+}-free (H_2SO_4 + $ZnSO_4$) electrolyte. Figure 8 presents the $V(t)$ recording obtained under these conditions. At the beginning of electrolysis, the anode potential was low, $V = 1.3$ V vs SSE, then increased during 1 h and stabilized at 1.49 V vs SSE for the remainder of the electrolysis. This value corresponds to that of a pure lead anode in Mn^{2+}-free electrolytes; potential oscillations never appear. Their existence requires both silver sites on the anode surface and Mn^{2+} ions in the solution.

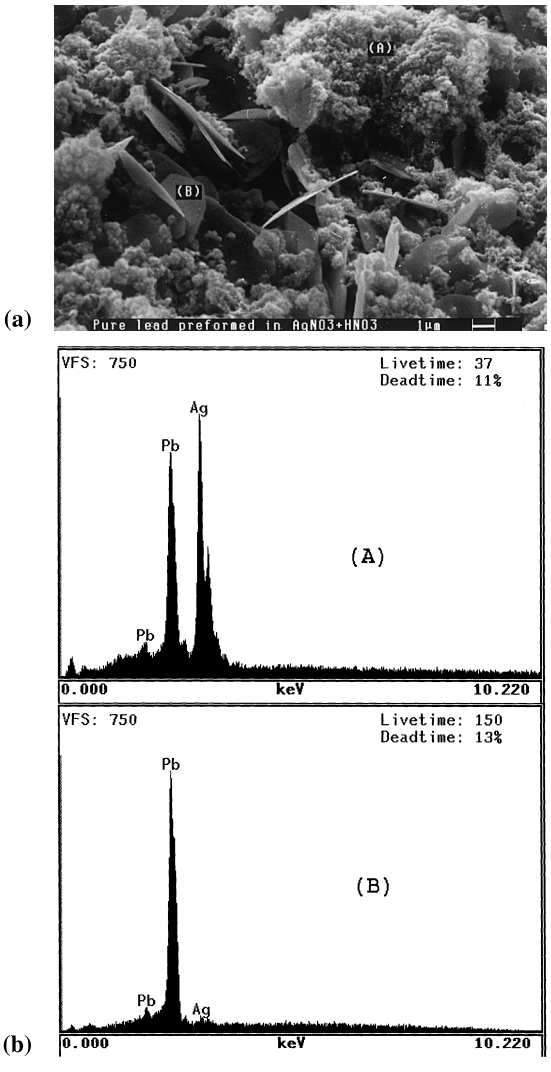

Fig. 6. SEM observation of the surface of a pure lead electrode preformed in the HNO_3 + $AgNO_3$ electrolyte. EDS spectra characteristic of silver sites (A) and lead matrix (B).

3.3. *Impedance spectra*

The time dependence of the electrode impedance spectra was examined under constant current density, at different stages of electrode ageing. During the induction time prior to oscillations the electrode impedance shows, at medium frequencies (Fig. 9, curve 1), a capacitive feature corresponding to inhibition by the silver salt adsorbate. An inductive behaviour also appears at low frequencies.

Later, when rare oscillations appear, the stability duration was sufficient to obtain impedance plots down to 80 mHz. Then the electrode impedance shows a negative resistance (Fig. 9, curve 2), indicating a much stronger inhibition at the electrode surface.

For well established potential oscillations, only truncated impedance plots (down to 0.2 Hz) could be recorded due to the limited duration of potential stability at the maximal value, V_{max}, and at the minimal value, V_{min}. As shown in Fig. 10, the impedance plots present two alternative shapes: plot 2 was obtained at V_{max} and plot 1 at V_{min}. These results indicate that the potential instabilities are due to periodic variations in the parameter responsible for the difference between the two plots in Fig. 9.

The potential oscillations observed in the present paper with lead–silver anodes can be explained in terms of the reaction model previously proposed from potentiostatic analysis of the electrochemical system [11]. The principal reaction is oxygen evolution, and secondary reactions associated to the formation of a silver salt adsorbate $(AgMnO_4^-)_{ad}$ occur on the MnO_2 layer existing on Pb–Ag electrodes, as indicated in Fig. 11. The rate constants, K_1 and K_2, of

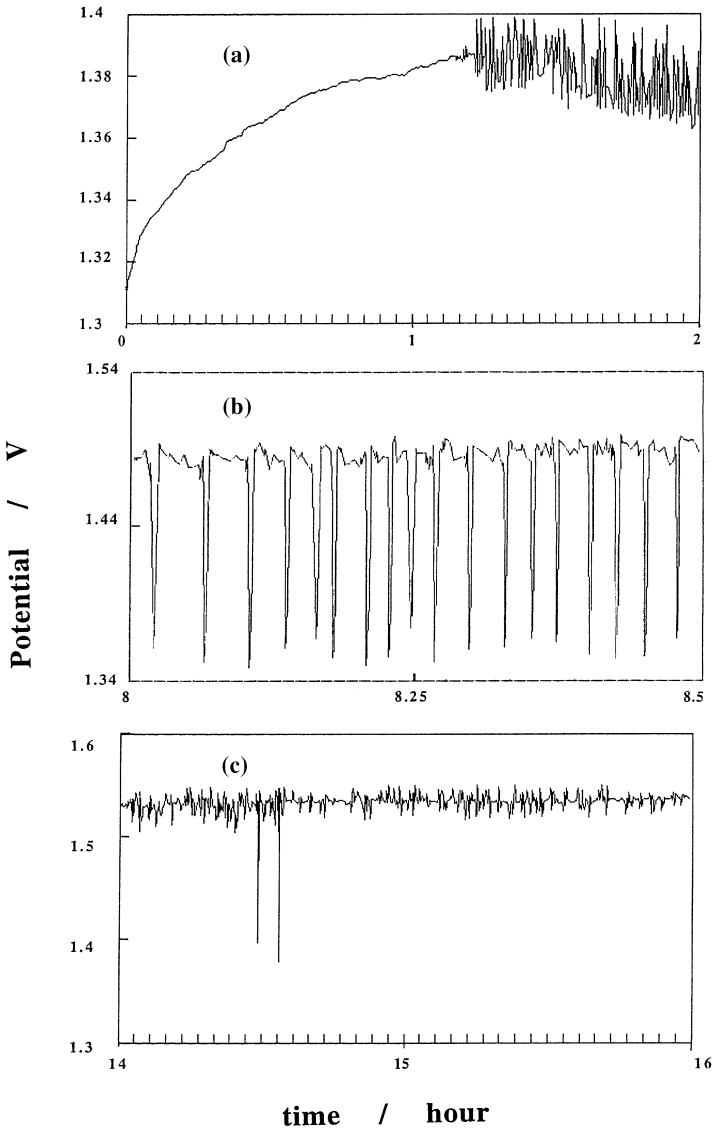

Fig. 7. $V(t)$ recording for a preformed lead anode, polarized at $i = 80\,\mathrm{mA\,cm^{-2}}$, in the H_2SO_4–$ZnSO_4$–$MnSO_4$ electrolyte, for different electrolysis times: (a) beginning; (b) 8 h; (c) 14 h.

the electrochemical steps are potential activated and the electrode coverage, θ, by the adsorbate is also potential activated. The relaxation of θ has been shown to give rise to the capacitive feature observed at medium frequencies on impedance plots [11]. It has also been shown that an increase in θ can generate a stronger inhibition and a negative resistance, R_o, as illustrated in Fig. 12. This Figure recalls the shape of typical impedance diagrams obtained at different

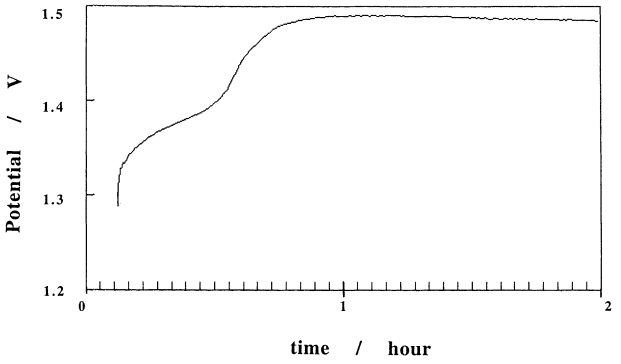

Fig. 8. $V(t)$ recording for a preformed lead anode, polarized at $i = 80\,\mathrm{mA\,cm^{-2}}$, in a Mn^{2+}-free electrolyte.

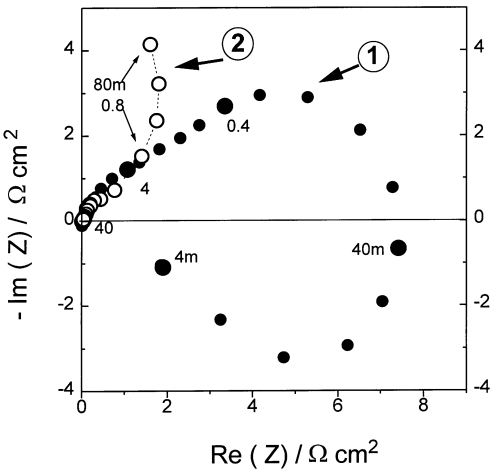

Fig. 9. Complex plane impedance plots (1) before (time: 15 min) and (2) at the beginning of ($t = 2$ h) oscillations; $i = 50\,\mathrm{mA\,cm^{-2}}$.

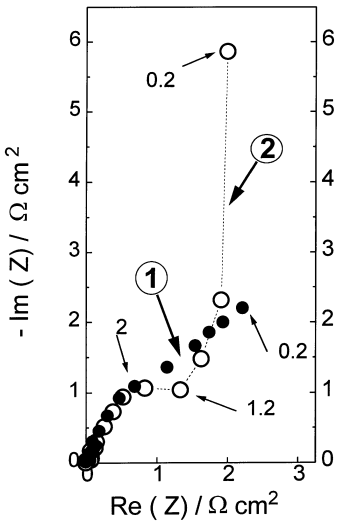

Fig. 10. Complex plane impedance plots during the oscillations.

potentials on the steady-state polarization curve plotted under potentiostatic conditions. The medium frequency capacitive feature corresponds to the relaxation of the electrode coverage, θ, whereas the low-frequency inductive loop is ascribed to the very slow relaxation of the conductivity of a sublayer of PbO or nonstoichiometric PbO_n present in the oxide layer [11, 17–19]. This inductive loop always extrapolates, at zero frequency, to a positive polarization resistance, in agreement with a polarization curve which remains single valued.

In terms of the model depicted in Fig. 11, the potential oscillations observed under galvanostatic conditions can be accounted for by considering periodic changes in the electrode coverage θ, by the adsorbate. These changes would be due to relatively fast breakdowns of the oxide layer, thus decreasing θ, followed by recovery of θ, taking place alternatively on the electrode surface. These breakdowns are likely triggered by the departure of large oxygen bubbles.

4. Conclusion

The kinetic behaviour of lead, and lead–silver alloy anodes, galvanostatically polarized in a H_2SO_4–$ZnSO_4$–$MnSO_4$ electrolyte under conditions similar to those industrially used for zinc electrowinning, have been compared. In this electrolyte, the potential of a lead anode remains stable during electrolysis. With lead–silver anodes, potential oscillations appear after an induction time of several hours. The shape and period of potential oscillations change with increasing time. Similar oscillations have also been observed with a pure lead electrode on which silver sites had been previously deposited, before using it as anode for zinc electrowinning. In addition to the presence of silver on the anode surface, the presence of Mn^{2+} ions in the electrolyte is necessary for the potential oscillations to appear.

Measurements of the electrolyte resistance during the formation of the PbO_2–MnO_2 layer reflect a change in the screening effect by bubbles. However,

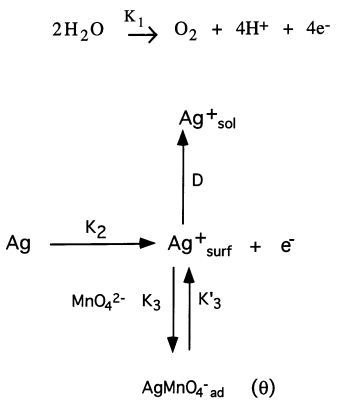

Fig. 11. Reactions taking place on Pb–Ag electrodes.

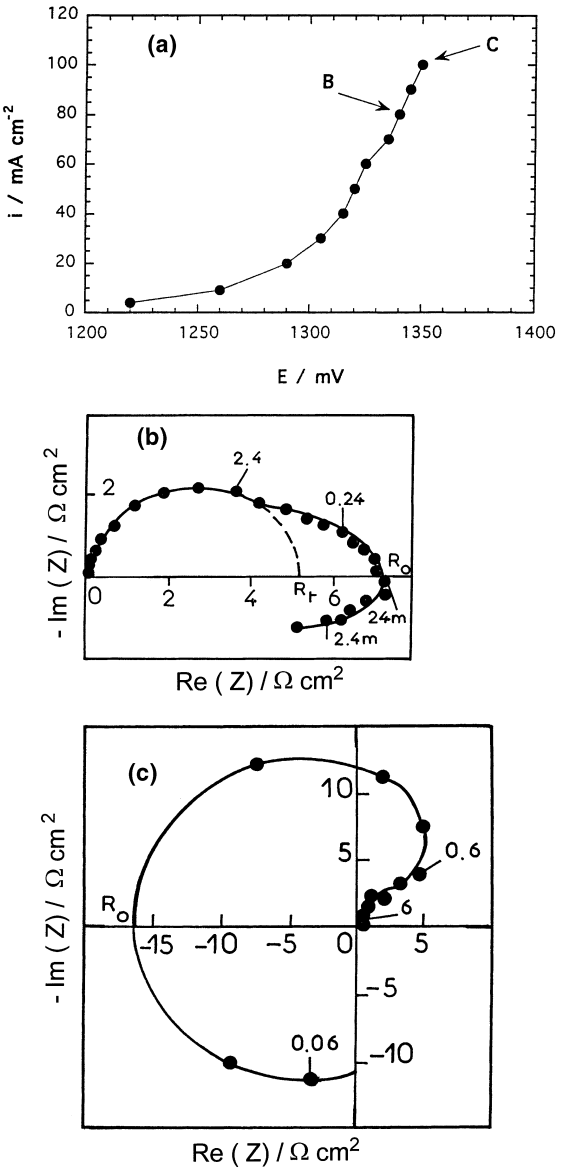

Fig. 12. (a) Typical steady-state polarization curve of Pb–Ag anode in the H_2SO_4 + $ZnSO_4$ + $MnSO_4$ electrolyte. Potentials are corrected for the ohmic drop iR_e. (B); (C): complex plane impedance plots measured at points B and C. R_t means charge transfer resistance.

the electrolyte resistance fluctuations are too small to account for the magnitude (about 100 mV) of the potential oscillations. From complex plane impedance plots determined before, at the beginning of, and during oscillations, it is concluded that the potential instabilities are due to periodic variations in the electrode coverage by a silver salt adsorbate present at the MnO_2-electrolyte interface.

Acknowledgements

Financial support by Union-Minière (France) is gratefully acknowledged.

References

[1] J. Wojtowicz, 'Modern Aspects of Electrochemistry', vol. 8 (edited by J. O'M. Bockris and B. E. Conway), Plenum Press, New York, (1972), p. 47.
[2] J. L. Hudson and T. T. Tsotsis, *Chem. Eng. Sci.* **49** (1994) 1493.
[3] D. Sazou, *Electrochim. Acta* **42** (1997) 627.
[4] C. Gabrielli and M. Keddam, *J. Electroanal. Chem.* **45** (1973) 267.
[5] M. Maja and P. Spinelli, *J. Electrochem. Soc.* **118** (1971) 1538.
[6] R. Wiart, C. Cachet, C. Bozhkov and S. Rashkov, *J. Appl. Electrochem.* **20** (1990) 381.
[7] Y. M. Wang, T. J. O'Keefe and W. J. James, *J. Electrochem. Soc.* **127** (1980) 2589.
[8] D. J. Mackinnon, R. M. Morrison and J. M. Brannen *J. Appl. Electrochem.* **16** (1986) 53.
[9] C. Cachet and R. Wiart, *J. Electrochem. Soc.* **141** (1994) 131.
[10] C. Cachet, C. Rérolle and R. Wiart, *Electrochim. Acta* **41** (1996) 83.
[11] C. Rérolle and R. Wiart, *ibid.* **41** (1996) 1063.
[12] P. J. Sides and C. W. Tobias, *J. Electrochem. Soc.* **129** (1982) 2715.
[13] L. J. J. Janssen and E. Barendrecht, *Electrochim. Acta* **28** (1983) 341.
[14] C. Cachet, M. Keddam, V. Mariotte and R. Wiart, *ibid.* **39** (1994) 2743.
[15] C. Gabrielli, F. Huet, M. Keddam, A. Macias and A. Sahar *J. Appl. Electrochem.* **19** (1989) 617.
[16] C. Gabrielli, F. Huet, M. Keddam, *J. Electrochem. Soc.* **138** (1991) L82.
[17] D. Pavlov, *Electrochim. Acta* **23** (1978) 845.
[18] P. Ruetschi and B. D. Cahan, *J. Electrochem. Soc.* **105** (1958) 369.
[19] F. Lappe, *J. Phys. Chem. Solids* **23** (1962) 1563.